

Modeling Wildland Fires: A Description of the Coupled Atmosphere- Wildland Fire Environment Model (CAWFE)

February, 2013

Janice L. Coen

NCAR Earth System Laboratory
Mesoscale and Microscale Meteorology Division

NCAR Technical Notes

**National Center for
Atmospheric Research
P. O. Box 3000
Boulder, Colorado
80307-3000
www.ucar.edu**



NCAR TECHNICAL NOTES

<http://www.ucar.edu/library/collections/technotes/technotes.jsp>

The Technical Notes series provides an outlet for a variety of NCAR Manuscripts that contribute in specialized ways to the body of scientific knowledge but that are not yet at a point of a formal journal, monograph or book publication. Reports in this series are issued by the NCAR scientific divisions, published by the NCAR Library. Designation symbols for the series include:

EDD – Engineering, Design, or Development Reports

Equipment descriptions, test results, instrumentation, and operating and maintenance manuals.

IA – Instructional Aids

Instruction manuals, bibliographies, film supplements, and other research or instructional aids.

PPR – Program Progress Reports

Field program reports, interim and working reports, survey reports, and plans for experiments.

PROC – Proceedings

Documentation or symposia, colloquia, conferences, workshops, and lectures. (Distribution maybe limited to attendees).

STR – Scientific and Technical Reports

Data compilations, theoretical and numerical investigations, and experimental results.

The National Center for Atmospheric Research (NCAR) is operated by the nonprofit University Corporation for Atmospheric Research (UCAR) under the sponsorship of the National Science Foundation. Any opinions, findings, conclusions, or recommendations expressed in this publication are those of the author(s) and do not necessarily reflect the views of the National Science Foundation.

National Center for Atmospheric Research
P. O. Box 3000
Boulder, Colorado 80307-3000
ISSN Print Edition 2153-2397
ISSN Electronic Edition 2153-2400

Modeling Wildland Fires: A Description of the Coupled Atmosphere-Wildland Fire Environment Model (CAWFE)

Janice L. Coen

NCAR Earth System Laboratory
Mesoscale and Microscale Meteorology Division

NCAR/TN-500+STR
NCAR Technical Note
Published By: NCAR Library
February, 2013

Contents

List of Figures	5
List of Tables	6
Acknowledgements	7
1. Introduction	8
2. Model components	9
2.1 Atmospheric model.....	10
2.2 Wildland fire module	12
2.2.1 Flaming front representation and tracking	14
2.2.2 Rate of spread of the flaming front	14
2.2.3 Post-frontal heat release	20
2.2.4 Partition into sensible and latent heat fluxes	21
2.2.5 Crown fire ignition and heat release	24
2.2.6 Smoke production	25
2.2.7 Upscaling and reintroduction of fire fluxes to the atmospheric model...	27
2.2.8 Implementation	27
3. Model initialization and experiment design	28
3.1 Atmospheric model initialization	28
3.2 Terrain	29
3.3 Fuel characteristics and condition	29
3.4 Experiment design	31
4. Model products	32
5. References	34

List of Figures

Fig. 1. Diagram of the CAWFE modeling system.

Figure 2. Green cells show the location of fuel cells (only the outermost, the most recently ignited, are shown). The tracer scheme that tracks the flaming front and identifies the burning region of each fuel cell. The component of the local wind vector (purple) in the direction of the unit normal vector (light blue) (pointing outward from the fire line (orange)) is used in calculating the local rate of spread of the interface.

Figure 3. The fraction of initial fuel remaining as a function of time after ignition time for rapidly burned fuel such as grass ($W=30$ s) and fuel with larger, slowly consumed components ($W=500$ s).

Figure 4. The effect of different values of W , the weighting factor, on fire behavior, for the 2 values of W given in Fig. 3. In the presence of 3 m s^{-1} winds from the left, rapidly-consumed fuels (upper left) create a fast-moving fire with heat fluxes distributed over a narrow burning depth (the thickness of the burning region) (upper right). In contrast, slowly-consumed fuels (lower left) create a slow-moving fire with lower heat fluxes distributed over a wider region (lower right). The color bar at right gives the sensible heat flux in kW m^{-2} .

Figure 5. This conceptual diagram contrasts (a) a widespread smoke modeling method, in which an assumed smoke profile (blue) is released in an atmospheric state unaltered by

fire, and (b) the approach of this modeling system, in which the model simulates the plume created by the fire and the time-dependent smoke release rates depending on the fuel consumption rate and variability in fire behavior. The dashed blue line represents the top of the atmospheric boundary layer, where an inversion capping vertical motion is often present and limits vertical exchange.

Figure 6. VAPOR visualization of the heat flux, near surface wind vectors, and smoke concentration during a CAWFE simulation of the 2006 Esperanza wildfire.

Figure 7. VAPOR visualization of the heat flux, near surface wind vectors, and smoke concentration during a CAWFE simulation of the 2012 High Park wildfire.

List of Tables

Table 1. Fuel models used by the fire behavior module.

Acknowledgements

This work describes the current contents of the Coupled Atmosphere-Wildland Fire Environment model (CAWFE), the fire module of which has been in development since approximately 1995. The fire module was originally conceived by Terry Clark (formerly of NCAR), with later contributions from Janice Coen (NCAR), Francis Fujioka (U.S.D.A. Forest Service Pacific Southwest Research Station), William Hall (NCAR), Don Latham (U.S.D.A. Forest Service Missoula Fire Laboratory), David Packham (Australian Bureau of Meteorology), and Philip Riggan (U.S.D.A. Forest Service Pacific Southwest Research Station).

Early model development was supported by the U.S.D.A. Forest Service Missoula Fire Laboratory and the U.S.D.A. Forest Service Riverside Fire Laboratory (now Pacific Southwest Research Station). This manuscript is based upon work supported by the National Science Foundation under Grants No. 0324910, 0421498, and 0835598, the Federal Emergency Management Agency under Award EMW-2011-FP-01124, and the National Aeronautics and Space Administration under Award 018568-001. The National Center for Atmospheric Research is sponsored by the National Science Foundation. Any opinions, findings, and conclusions or recommendations expressed in this material are the author's and do not necessarily reflect the views of the National Science Foundation.

1. Introduction

Our ability to learn from previous wildland fire events is limited by our understanding about how factors such as evolving weather, fuels, and terrain combine, and why.

Operational fire behavior models such as BehavePlus (Andrews 2009) or FARSITE (Finney 1998), which are used by land management agencies to simulate fire spread across landscapes, attempt to do so by considering weather, terrain, and fuels as external, independent variables. These ‘kinematic’ models do not consider the dynamical forces involved, such as the acceleration of air due to pressure gradients, buoyancy created by vertical motion of stratified air, or the heat released by a fire.

In contrast, coupled weather-wildland fire models, which join full weather prediction models interactively with fire behavior models, aim not only to simulate the direction and rate of fire spread, but to describe the interacting dynamical forces that determine a fire’s evolution, reproduce characteristic phenomena, and provide understanding why each fire unfolds in the unique way that it does. This work describes the Coupled Atmosphere-Wildland Fire-Environment (CAWFE) model and how it simultaneously models the evolving meteorological flow, fire behavior, and fire-induced winds. CAWFE ties a numerical weather prediction model to components representing the spread of a wildland fire and consumption of wildland fuels to simulate the impact of a fire on the atmosphere and the subsequent feedback of these fire-altered winds on fire behavior - i.e. how all fires, to some degree, 'create their own weather'. As such, CAWFE aims to reproduce fire growth in spatially varying and potentially reinforcing fuel, weather and terrain conditions, but more importantly, reproduce fire phenomena and

provide understanding about the mechanisms that create the uniqueness of each wildland fire event.

2. Model components

The CAWFE modeling system is composed of two parts, a numerical weather prediction model and a fire behavior module that models the growth from ignition, propagation, and decay of a wildfire in response to terrain, fuel, and evolving weather and fuel conditions.

The atmospheric model, described below, was developed over two decades to study weather evolution over complex terrain, including precipitation formation, downslope windstorms, cloud entrainment, weather modification, clear air turbulence, and terrain-induced turbulence. More recently, a component that represents the growth of a wildland fire in response to factors in the fire environment such as wind, terrain, and fuels, and the fire's impact on the atmosphere was added. This document primarily describes the fire module as implemented in CAWFE, the coupling between the components, and relevant aspects in the atmospheric model; the reader is referred to prior works for details of the atmospheric model. Many components of CAWFE's fire module, with some modifications and additions from other contributors, are now distributed in the Weather Research and Forecasting (WRF) model as the physics package WRF-Fire, which is described in Coen et al. (2013). Therefore, the CAWFE model description in this section is similar to the WRF-Fire model description in Coen et al. (2013), which describes their differences.

The fire behavior module in CAWFE is two-way coupled to the atmospheric model: low level winds drive the spread of the surface fire, which releases sensible heat,

latent heat, and smoke into the lower atmosphere. Surface heat fluxes vary in space and time according to the rate at which fuel is consumed, and in turn, feed back to affect the winds directing the fire. This modeling system can thus represent the complex interactions between a fire and the atmosphere. Although this influence is most dramatic near the fire, model simulations show a wildland fire can change the wind speed by several kilometers per hour even several kilometers distant from the fire (Coen 2005). CAWFE does not explicitly simulate flames or combustion, instead it parameterizes these processes with scale-commensurate semi-empirical and empirical relationships -- the simulated atmosphere responds to the fire's sensible heat (temperature), latent (water vapor) heat, and smoke fluxes, which vary in space and time in accordance with the rate at which fuel is consumed.

2.1 Atmospheric model

The Clark-Hall meteorological model is a three-dimensional, non-hydrostatic numerical weather prediction model. The atmospheric model's governing equations, parameters, flow structures, nesting procedures, their representation in discretized form, and physical parameterizations were described in a prior Technical Note (Clark et al. 1996a). Other works (Clark 1977, 1979; Clark and Farley 1984; Clark and Hall 1991, 1996; Clark et al. 1996a, 1997) detail different aspects of the model.

The model is comprised of the prognostic Navier-Stokes equations of motion, a thermodynamic equation, the continuity equation formulated with the anelastic approximation (Ogura and Phillips 1962) for the conservation of mass, and prognostic equations for the concentrations of atmospheric water vapor, cloud water, rain water, ice

crystals, and rimed ice hydrometeors. Vertically stretched terrain-following coordinates allow the model to simulate the detailed airflow over complex terrain. Gridded domains with two-way interactive nesting capture the synoptic-scale outer forcing in the outer domain while allowing the simulation to telescope down to tens of meters near the fireline through horizontal and vertical grid refinement (Clark and Hall 1996). Thus, the numerical weather prediction model can model fine scale atmospheric flows (with horizontal resolution of tens to hundreds of meters) in very steep terrain where the slope may exceed 30° .

A sequence of three-dimensional states of the larger-scale atmospheric environment from either gridded atmospheric analyses or a model simulation are used to initialize the outermost domain and provide lateral boundary conditions throughout a CAWFE simulation. The coarse meshes contain no turbulence and no parameterization of boundary layer fluxes is performed, while the finest meshes may be turbulence resolving. Small-scale shear-driven and convective turbulent motions are modeled explicitly by the model (Clark et al. 1997) down to the grid resolution (the “large eddy simulation” (LES) approach). As detailed in Clark et al. (1997), the Smagorinsky (1963) and Lilly (1962) schemes treat subgrid-scale closure of the eddy mixing coefficients with Prandtl and Richardson number dependence, in which the eddy length scale in the atmospheric boundary layer is calculated using the Blackadar (1962) formulation. A consequence of this approach is that the inflow boundary conditions for turbulence-resolving domains are laminar and eddies have limited time to spin-up. This is in contrast to true LES simulations, which use periodic boundary conditions to allow turbulence to fully develop, but are limited to somewhat idealized experiments.

Weather processes such as the production, interaction, sedimentation, and evaporation or melting of cloud droplets, rain, and ice are parameterized using standard microphysical parameterizations (Clark et al. 1996a).

2.2 *Wildland fire module*

The wildland fire module represents the ignition, propagation, and decay of a wildland fire propagating through surface fuels such as grass, shrubs, and vegetation litter. If an overlying canopy is present and the surface fire intensity exceeds a given threshold, the surface fire may heat, dry, ignite, and consume the canopy. A sequence of previous work (Clark et al. 1996b, 1996c, 2004; Coen 2005) developed the treatment of physical processes; the current methods and connection to the atmospheric model are summarized here. Four components treat physical processes including the flaming front's rate of spread, post-frontal heat release, crown fire ignition and consumption, and upscaling of heat release into the atmospheric model, and an additional algorithm defines the subgrid-scale interface between burning and unignited fuel. A diagram of the components is given in Fig. 1. CAWFE is designed to resolve atmospheric motions from tens of meters to hundreds of kilometers, while wildland fire physical processes occur at scales several orders of magnitude smaller than the atmospheric grid size. Thus, CAWFE does not explicitly simulate flames or combustion chemistry. Neither the fuel temperature, fire temperature, nor the consumption of oxygen or flammable pyrolyzed gases is tracked by this model. Instead, CAWFE parameterizes these subgrid-scale processes by adapting scale-commensurate semi-empirical and empirical relationships, i.e. ones that represent the effect of the fire on the atmosphere at the scales of motion that the model resolves.

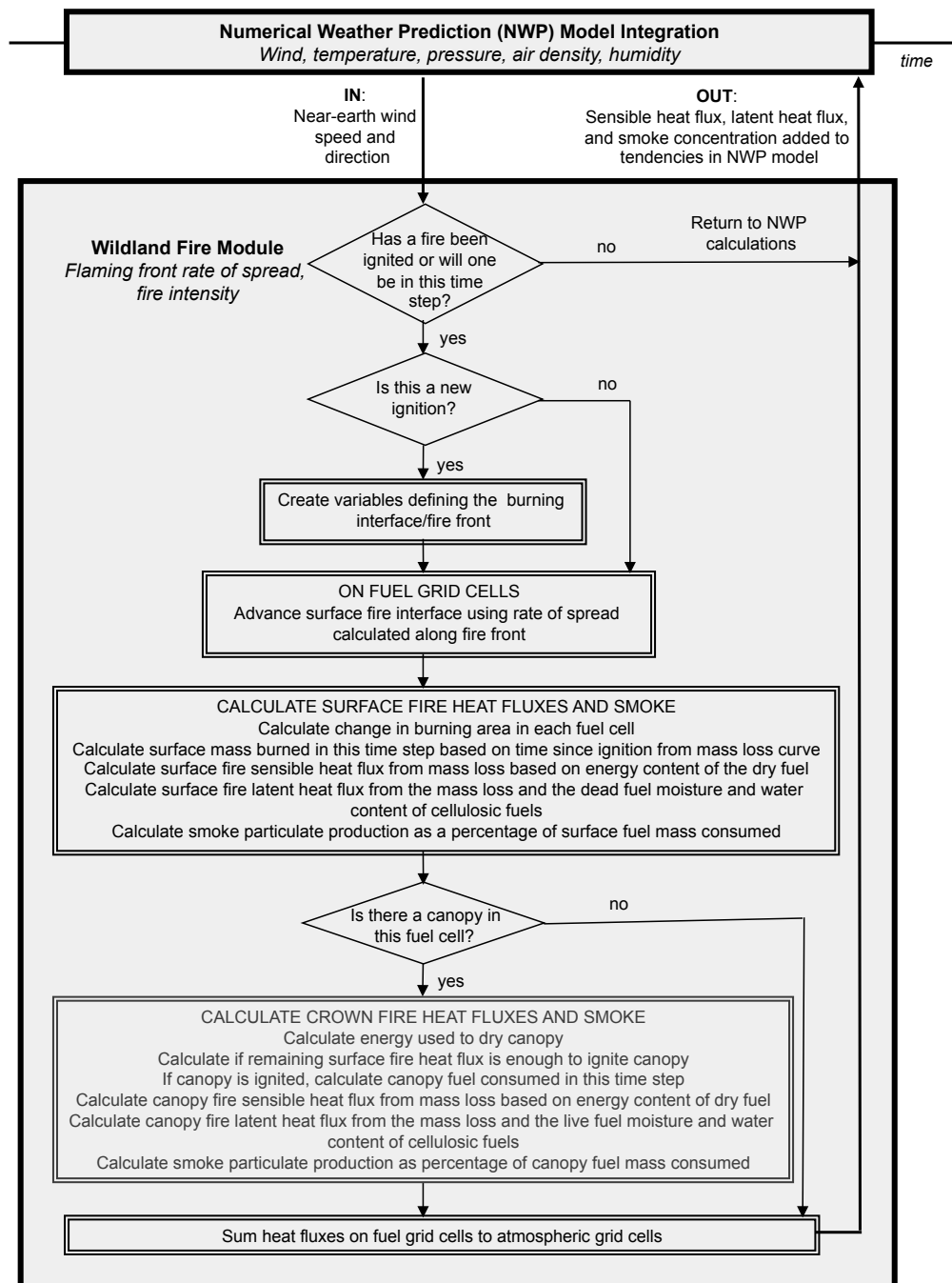


Figure 1. Diagram of the CAWFE modeling system.

Long-range spotting, in which burning embers may be lofted by the fire plume and drop many kilometers downwind, igniting new fires, is also not treated by the model.

2.2.1 Flaming front representation and tracking

In a two-dimensional plane at the earth's surface, each atmospheric grid cell is further subdivided into higher-resolution two-dimensional rectangular fuel cells, with fuel physical characteristics and fuel loads specified by the user (see Section 3.3).

Although model fuel cells may be a few to hundreds of meters in size, the interface between burning and unignited fuel results from complex subgrid-scale nonlinear fluid dynamics and thus is smaller than even these fuel cells can resolve. Clark et al. (2004) described the front-tracking scheme in CAWFE that represents the fire front interface as it passes through fuel cells. Within each fuel cell lie four tracers, which are moving points that represent the interface between burning and non-burning areas within the fuel cell. Viewed together with neighboring cells, these tracers define the fire front. A sample simulated fire front (Fig. 2) shows the complexity that may evolve in the shape of a fire. A local contour advection scheme assures consistency between grid cells along the fireline.

2.2.2 Rate of spread of the flaming front

The Rothermel (1972) algorithms, as restated in metric units by Wilson (1980), are used to parameterize the fire's rate of spread in terms of characteristics in the fire environment. Fire spread rates normal to the interface are calculated locally along the fire front as a function of fuel properties, the wind component from the atmospheric model, and the

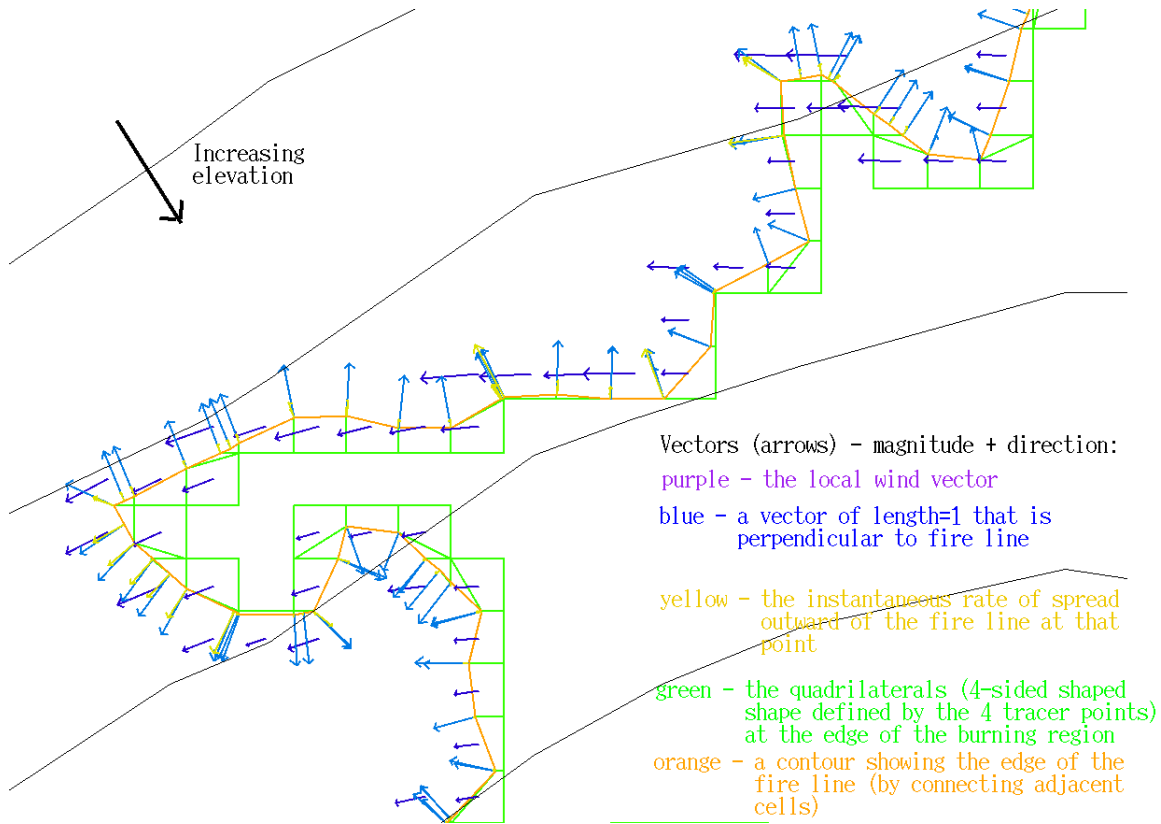


Figure 2. Green cells show the location of fuel cells (only the outermost, the most recently ignited, are shown). The tracer scheme that tracks the flaming front and identifies the burning region of each fuel cell. The component of the local wind vector (purple) in the direction of the unit normal vector (light blue) (pointing outward from the fire line (orange)) is used in calculating the local rate of spread of the interface.

terrain slope, the latter two both taken normal to the fireline. This rate is assumed to represent the effects of all processes that propagate the fire, including radiation heating, drying, and igniting unburned fuel, convective heating, contact ignition, and the spotting of small flaming embers short distances ahead of the fireline. The model applies the semi-empirical point-based algorithm (Rothermel 1972), developed for fuel complexes in

the United States, which relates the rate of spread of the flaming front to local wind, terrain slope, and a set of fuel characteristics for each fuel type:

$$R = R_o(1 + \Phi_s + \Phi_w) \quad (1)$$

Equation (1) is semi-empirical: the rate of spread of the leading edge of the flaming front (m s^{-1}), is related to a base theoretically-determined rate of spread, R_o , which is a function of fuel properties only in zero wind conditions on flat ground. These were calibrated to small flame experiments in a chamber where the wind speed and slope were varied using empirically determined functions of terrain slope, Φ_s (dimensionless), and wind speed, Φ_w (dimensionless). Each of these terms is a function of other properties. We refer the reader to the Appendix in Rothermel (1972) for details; we repeat here only what is needed for discussion or calculated or applied differently from the original.

The term R_o is calculated as:

$$R_o = \frac{I_R \xi}{\rho_b \varepsilon Q_{ig}} \quad (2)$$

in which I_R is the reaction intensity (W m^{-2}), the rate of heat release per unit area per unit time in the fire; ξ is the propagating flux ratio (dimensionless); ρ_b is the oven dry bulk density (kg m^{-3}), the mass of fuel per cubic meter of fuel bed; ε is the effective heating number (dimensionless); and Q_{ig} is the heat of preignition (J kg^{-1}), the amount of heat required to heat 1 kg of fuel to combustion temperature. Equation (2) can be interpreted to mean that the rate of spread is related to the ratio of the amount of heat received by the fuels ahead of the flaming zone (the numerator) tempered by the amount of heat it takes to raise the fuel to combustion temperatures (the denominator).

The wind coefficient Φ_w is calculated as in Rothermel (1972):

$$\Phi_w = CS^B \left(\frac{\beta}{\beta_{op}} \right)^{-E} \quad (3)$$

where S is the magnitude of the component of the wind velocity normal to the fire line.

The coefficients C , B , and E , and optimum packing ratio β_{op} are calculated as in

Rothermel (1972), as functions of the surface area to volume ratio of the fuel complex, and the packing ratio β (dimensionless) relates the density of the fuel complex to the density of the fuel particles themselves. When the component of wind normal to the fire line is directed into the fire, the backing rate of spread in these experiments is 0 for chaparral and other shrubs, as backing is not observed to occur, and 0.003 m s^{-1} in other surface fuel models.

Observations and experimental evidence (e.g. Riggan et al. 2010) shows that fire spread in southern California chaparral fuels primarily depends on ambient winds rather than the particulars of fuel loadings and does not respond to environmental factors as the Rothermel (1972) relationship states. Therefore, an alternative relationship (Clark et al. 2004) is available in the model:

$$R = 1.2974 S^{1.41} \quad (4)$$

where R and S are in m s^{-1} . When the wind component normal to the fire line points into the fire, the backing rate of spread is zero, since chaparral requires wind directing flames into unignited fuel to maintain flame propagation.

An alternative relationship (Noble et al. 1980) is available for Australasian fuel complexes:

$$R = 0.18 e^{0.8424 S} \quad (5)$$

where R and S are in m s^{-1} . When the wind component normal to the fire line is directed into the fire, the backing rate of spread is 0.18 m s^{-1} .

We assume that the rate of spread of a heading fire given by (1), (4), or (5) can be applied to landscape-scale fires within a wide range of conditions (wind speeds less than 30 m s^{-1}) some of which are outside the range of laboratory or small fire experimental conditions on which the equations are based. We also assume that the fire propagation speed normal to the interface can be calculated at all points along the fire front using (1), local fuel properties, and wind at an appropriate location from the atmospheric model and the local terrain slope, both normal to the fireline.

Choosing the location of the wind driving the fire is an area of active research. A difference here from the use of Rothermel (1972) in its original form and in kinematic models such as BehavePlus (Andrews 2009) or FARSITE (Finney 1998) is that the wind driving the fire has been modified by feedbacks from the fire. It is widely recognized that winds are a dominant factor in fire behavior, with increasing wind speeds increasing the rate of spread. In developing a formula for the quasi-steady state rate of fire spread, Rothermel (1972) assumed a uniform ambient wind that, in principle, was driving the fire and heuristically reduced winds to an estimated midflame height. More recent perspectives recognize the spatial variability of winds and the fire's dramatic shaping of winds in its environment (e.g. Clark et al. 1996b, 1996c). As a strong heat source imparts a strong vertical component to air velocity, the horizontal wind speed can go to zero at the confluence of winds into the updraft, which may tilt ahead of, over, or behind the fire line. On the Clark-Hall model's Arakawa C-grid, the latitudinal and meridional horizontal wind components are located on the midpoints on the east and north sides,

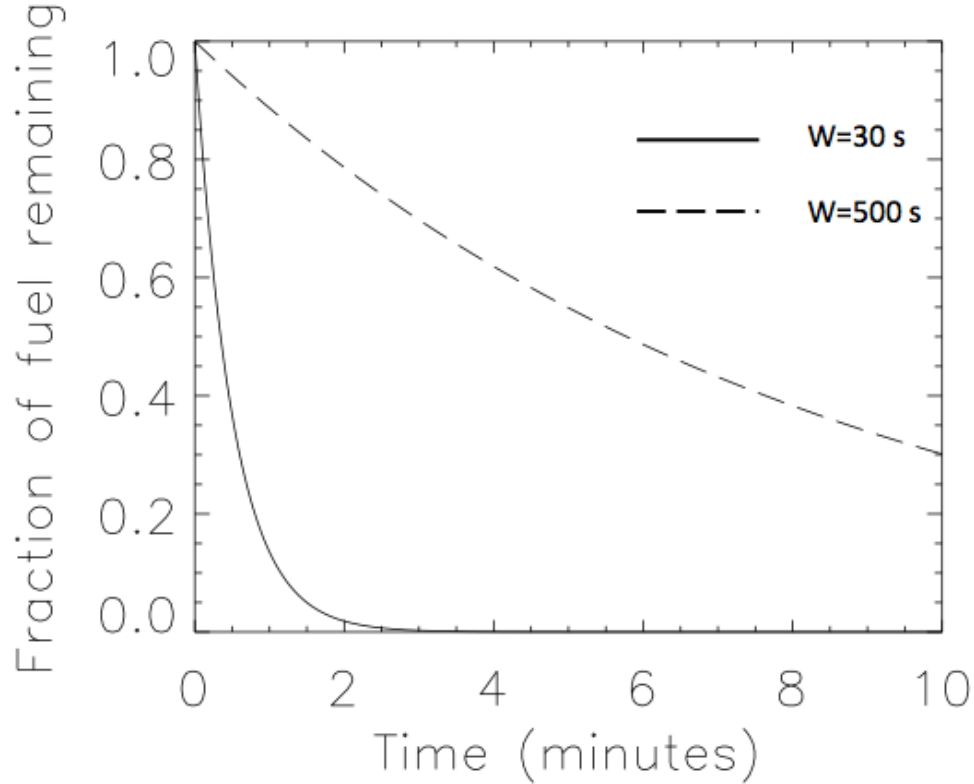


Figure 3. The fraction of initial fuel remaining as a function of time after ignition time for rapidly burned fuel such as grass ($W=30$ s) and fuel with larger, slowly consumed components ($W=500$ s).

respectively, of the atmospheric grid cells. These wind components are interpolated horizontally to a user-chosen distance behind the fireline and vertically using the log wind profile (Oke 1987) to the fuel bed's height where the component normal to the fireline is used in the rate of spread calculation. The mechanisms through which wind affects a fire's rate of spread and how it should be incorporated in models remain active research areas.

2.2.3 *Post-frontal heat release*

CAWFE uses a semi-empirical algorithm based on laboratory experiments to calculate the post-frontal heat release rate that characterizes how rapidly fire consumes fuels of different sizes with time after ignition, distinguishing, for example, between rapidly consumed grasses and slowly burned woody stems or logs (Fig. 3). This algorithm assumes an exponential depletion of fuel mass from the time of ignition, calibrated for various fuel types burned in laboratory fuel consumption experiments. The fuel consumption rate is controlled with a weighting parameter, W , that characterizes the time (s) required for the fuel load to decrease to a factor of e^{-1} of the original load (Coen 2005):

$$1 - F = \exp\left(\frac{-t}{W}\right) \quad (6)$$

where F is the fraction of fuel that has been burned and t is the time since ignition. Values of W , based on the experiments of Albini (1994) and Albini et al. (1995), are given in Table 1. Figure 4 shows the effect of W on fire behavior. Rapidly consumed (low- W) fuels create a fast-moving fire with heat fluxes distributed over a narrow burning depth (the thickness of the burning region), while slowly-consumed (high- W) fuels create a slow-moving fire with lower heat fluxes distributed over a wider region. The fire stops releasing heat when the remaining fuel approaches an infinitesimally small amount or the fuel moisture exceeds that fuel category's moisture content of extinction.

Because the fireline propagates through a fuel cell, points within a cell will have been burning for different lengths of time. To determine the mass of fuel lost, Clark et al. (2004) developed formulas that estimated the time history of the area burned in the fuel

cell and, from that, calculated how much fuel was consumed in the current time step. If the fuel cell is instantly totally burning,

$$\Delta m = f_i \left(1 - e^{-\frac{t_{crit}}{w}} \right) \quad (7)$$

where Δm is the change in mass in this cell during the current time step, f_i is the initial fuel load, and t_{crit} is the first time since cell ignition at which the whole cell is burning. If the cell is ignited but not yet fully ignited:

$$\Delta m = f_i A \left(1 + \frac{w}{t_{cell}} \left(e^{-\frac{t_{cell}}{w}} - 1 \right) \right) \quad (8)$$

where t_{cell} is the time since the cell first ignited and A is the fractional cell area that is burning, which ranges from 0 (not burning) to 1 (fully burning). If the fuel cell has become fully burning:

$$\Delta m = f_i \left[A \left(1 + \frac{w}{t_{crit}} \left(e^{-\frac{t_{crit}}{w}} - 1 \right) \right) + \frac{w}{t_{crit}} \left(1 - e^{-\frac{t_{crit}}{w}} \right) \left(1 - e^{-\frac{t_{crit}-t_{cell}}{w}} \right) \right] \quad (9)$$

2.2.4 Partition into sensible and latent heat fluxes

Sensible and latent heat fluxes are calculated in each fuel grid cell. Based on the energy content of dry fuel, the mass loss rate is converted to an energy release rate (J s^{-1}) which is summed over each fuel cell's area to give the sensible heat flux. The sensible heat flux H_s (in W m^{-2}) released by the ground fire is calculated as

$$H_s = \frac{\Delta m}{\Delta t} (1 - B) h_c \quad (10)$$

where Δm is the change in fuel load (kg m^{-2}) in the current time step, Δt , h_c is the heat of combustion (J kg^{-1}) for dry cellulose fuels (17.4 MJ kg^{-1}), B is the fraction of the total

Table 1. Fuel models used by the fire behavior module. Columns show fuel properties associated with each fuel model.

Fuel model	Name	Surface fuel load (kg m ²)	Weighting parameter, W (s)	Surface area to volume ratio, σ (m ⁻¹)	Fuel depth (m)	Fuel moisture content of extinction	Canopy fuel load (kg m ²)	Canopy fuel burnout time (s)
1	Short grass	0.167	7.	11483.	0.305	0.12	0.	--
2	Grass + understory	0.896	30.	7500.	0.610	0.15	0.	--
3	Tall grass	0.674	7.	4921.	0.762	0.25	0.	--
4	Chaparral	3.591	360.	4400.	2.000	0.20	0.	--
5	Brush	0.784	360.	5100.	0.667	0.20	0.	--
6	Dormant brush, hardwood slash	1.344	360.	5131.	0.762	0.25	0.	--
7	Southern rough	1.091	360.	5125.	0.762	0.40	0.	--
8	Closed timber litter	1.120	1200.	2089.	0.061	0.30	1.121	60.
9	Hardwood litter	0.780	1200.	6916.	0.061	0.25	1.121	120.
10	Timber litter + understory	2.692	1200.	2089.	0.305	0.25	1.121	180.
99	No vegetation	0.000	--	--	--	--	--	--

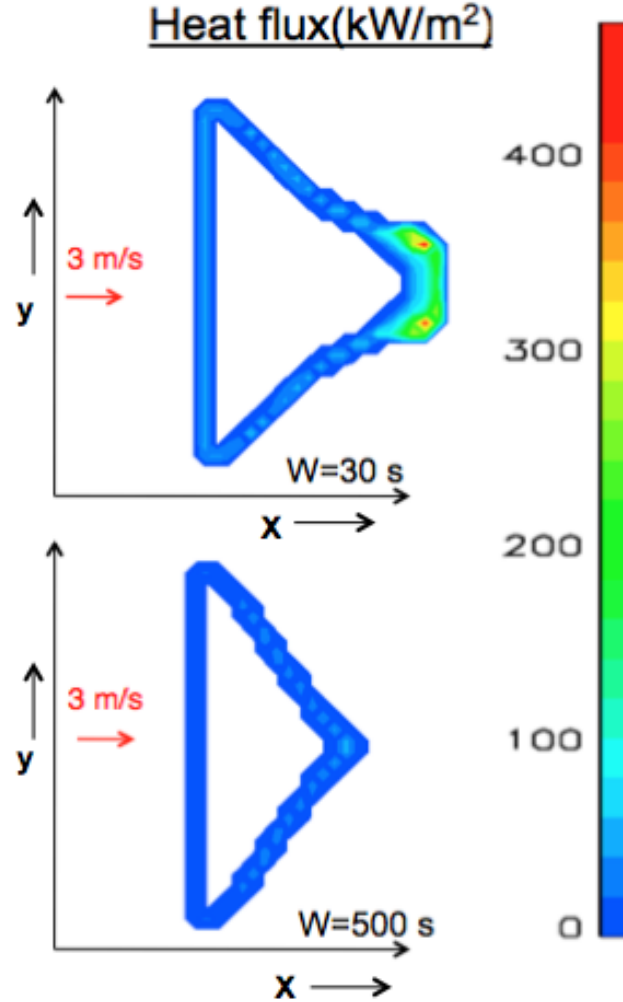


Figure 4. The effect of different values of W , the weighting factor, on fire behavior, for the 2 values of W given in Fig. 3. In the presence of 3 m s^{-1} winds from the left, rapidly-consumed fuels create a fast-moving fire with heat fluxes distributed over a narrow burning depth (the thickness of the burning region) (upper figure). In contrast, slowly-consumed fuels create a slow-moving fire with lower heat fluxes distributed over a wider region (lower figure). The color bar at right gives the sensible heat flux in kW m^{-2} .

fuel mass that is water. The term B is related to the more commonly measured fuel moisture content, FMC, the mass of water per unit mass of dry fuel, by:

$$B = \frac{FMC}{1 + FMC} \quad (11)$$

Combustion releases water absorbed by the fuel from its environment (the fuel moisture content), which varies with ambient conditions for dead fuels and with the plant health and drought stress in live fuels. Combustion also releases water bound in cellulose, which is assumed to make up 56% of the biomass. The latent heat flux liberated by combustion is calculated based on the mass consumed in the current time step, the fuel moisture content for either dead or living fuel, and the water content of cellulosic fuels. The latent heat flux LE_s released by the surface fire is calculated as:

$$LE_s = \frac{\Delta m}{\Delta t} [B + 0.56(1 - B)]L_v \quad (12)$$

where L_v is the latent heat of vaporization of water (J kg^{-1}). The first term in parentheses arises from the water absorbed by the fuel from its environment and held between the cellulose cells of wood, the second term accounts for the water bound in the cellulose fuel cells themselves.

2.2.5 *Crown fire ignition and heat release*

Energy from the surface fire is first used to heat and dry any canopy above a surface fire. Following Van Wagner (1977), the canopy is ignited if the residual heat flux, after heating and drying the canopy, exceeds a threshold value, specified in this model as 170 kW m^{-2} . Once ignited, we assume that the canopy mass decreases linearly over the canopy burnout time (see values in Table 1). Based on the energy content of dry fuel, this rate of energy release is converted to an energy release rate per unit area, or crown fire

sensible heat flux. Then, based on the canopy's mass loss, live fuel moisture, and the water content of cellulosic fuels, a latent heat flux is calculated using (12). A crown fire, if it is modeled to occur, is assumed to remain collocated with the surface fire due to the transient nature of running crown fires (D. Sandberg, personal communication).

2.2.6 Smoke production

As a simple representation of smoke, it is assumed that 2% of the mass consumed by both the surface and crown fires becomes particulate matter that has no fall speed with respect to air nor does it impact other physics processes such as radiation but is transported by the atmospheric model similarly to the other scalars. The smoke mass concentration from the surface (crown) fire is added to the lowest (two lowest) atmospheric grids, respectively, and transported upwards in the fire plume, diffused by mixing of the plume with ambient air and distributed by the atmospheric circulation.

The model is thus able to represent the production rate of particulates in response to fire intensity and burning rates, how these rates respond to fuel, terrain, and atmospheric factors, and how they vary throughout the day and at different locations along the fire. CAWFE treats the transport of smoke differently than current operational air quality tools (Fig. 5), which may distribute a vertical profile of particulates in the three-dimensional wind field of an atmospheric model or analysis to mimic the vertical transport of the fire plume. In contrast, by explicitly simulating the buoyancy and updraft created by the fire, CAWFE can reproduce when and how much smoke is lofted from the atmospheric boundary layer into usually stronger middle-atmospheric winds that can sometimes transport smoke thousands of kilometers.

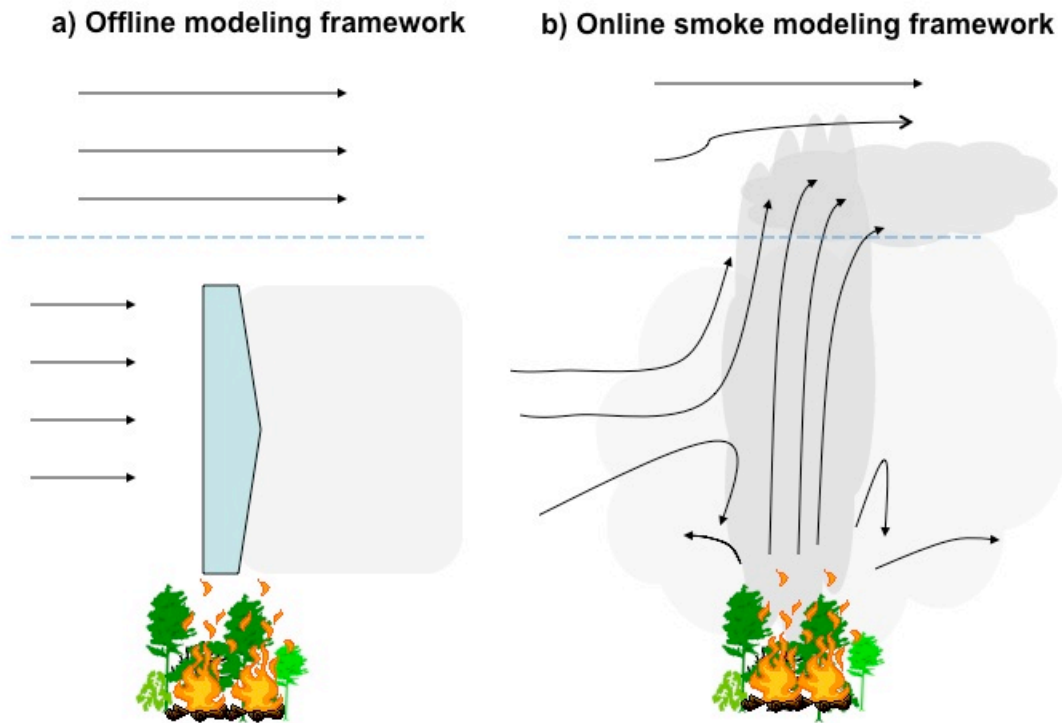


Figure 5. This conceptual diagram contrasts (a) a widespread smoke modeling method, in which an assumed smoke profile (blue) is released in an atmospheric state unaltered by fire, and (b) the approach of this modeling system, in which the model simulates the plume created by the fire and the time-dependent smoke release rates depending on the fuel consumption rate and variability in fire behavior. The dashed blue line represents the top of the atmospheric boundary layer, where an inversion capping vertical motion is often present and limits vertical exchange.

2.2.7 Upscaling and reintroduction of fire fluxes to the atmospheric model

The sensible and latent heat fluxes produced by the fire are summed horizontally from fuel grid cells to the atmospheric cells and returned to the numerical weather prediction model. There, they are distributed vertically through an empirically estimated extinction depth in the innermost domain. As supported by experimental data in Coen et al. (2004) and Clements et al. (2007), the extinction depth concept is based on the assumption that a simple radiation treatment could be used to distribute the sensible and latent heat and smoke into the lowest atmospheric grid levels. The e-folding height over which the heat is distributed in the atmospheric model (α_s) is typically specified as 10 m for grass fires, based on data in Clements et al. (2007), and 50 m for crown fires, based on analysis of infrared observations of wildfires (Coen et al. 2004). The heat fluxes become additional tendencies to the potential temperature and water vapor prognostic equations in the innermost domain of the atmospheric model, altering the atmospheric state. Although the fire is treated only in the innermost mesh, the effects of the fire on the atmospheric state may be seen in the outer meshes through the grid nesting procedure, which exchanges information between coarser and finer domains.

2.2.8 Implementation

During each time step, the interface between burning and unignited fuel (the fire front) advances into fresh fuel while previously ignited areas consume more fuel. The atmospheric and fire model components exchange information as heat and water vapor fluxes from the fire alter the atmospheric state, notably producing fire winds, while the

updated atmospheric state and changes in humidity (including effects from the fire) in turn affect fire behavior, specifically, how fast and in what direction the fire propagates.

The model can run on a relatively coarse grid, with the fuel grid size dictated only by desired resolution in the fire region and a requirement that the fire not cross more than one cell during a time step, however the fire's effects on the atmospheric winds become more dilute with coarser atmospheric grid spacing. We note that the fire component cannot realistically be run separately without two-way coupling to the atmospheric component. Models without coupling (i.e. FARSITE) are required to impose an additional constraint, a shape on the fireline, as otherwise a line ignition would spread simply in a line, which is not realistic. The coupling constrains the wind near the fireline, becoming the constraint required to produce a realistic fire shape. This has a stabilizing effect – winds are drawn parallel to the flanks, discouraging outward growth, toward the heading region. If the grid resolution is high enough, perturbations along the flank may spin up as fire whirls and be transported downwind along the fire's edge toward the head.

3. Model initialization and experiment design

To perform an experiment, the atmospheric initial state, terrain elevation, fuel state, and two-dimensional map of fuel properties are gathered, along with the ignition time and location.

3.1 *Atmospheric model initialization*

Large-scale gridded atmospheric analyses or model output, such as a Weather Research and Forecasting (WRF) model regional weather simulation spanning the period before

and during the fire, provides initial conditions and boundary conditions for the finer resolution CAWFE model simulation. To do so, the three-dimensional gridded data is interpolated onto the CAWFE three-dimensional grid at the beginning of the CAWFE simulation. Data at later times is used to specify lateral boundary gradients of winds, temperature, and other atmospheric state variables in the outermost CAWFE domain at approximately 1-6 h intervals.

3.2 *Terrain*

Terrain data covering the United States is freely available from <http://nationalmap.gov>. The terrain for the modeling domains is sampled from 0.33, 1, and 3 arc second terrain elevation data smoothed with one pass of a 1-2-1 bidirectional filter to remove high frequency noise.

3.3 *Fuel characteristics and condition*

Fuel properties are commonly specified using stylized fuel categorization schemes (“fuel models”) such as those of Anderson (1982) or Scott and Burgan (2005). These fuel categorization schemes group together fuels with similar fire behavior properties and assign a category (and an associated fixed set of properties including fuel load, arrangement, and physical composition) based on anticipated burning behavior. As a default for experiments, the spatial distribution of fuel properties in the innermost modeling domain is categorized by the 13 fire behavior fuel models compiled by Rothermel (1972) and Albini (1976), as restated with pictures by Anderson (1982), and referred to herein as the Anderson fuel models.. Data is obtained from LANDFIRE’s

geospatial database (LANDFIRE 2007), which was developed from satellite remote sensing data improved by limited in situ sampling. Anderson Fuel Model 4, one of 13 fuel models, is widely and uncritically applied to chaparral while Fuel Model 5 has been applied to younger chaparral with little dead fuel. The fuel properties associated with these fuel models, along with additional fuel model-specific properties needed for this dynamic model, are given in Table 1. These additional fuel properties include a weighting function, $W(s)$, for each fuel model that defines how rapidly the mass loading decreases with time once ignited. Another property specific to this model is α_s and α_c , the vertical depths over which the heat released from the surface and crown fires are released, respectively, which are set to 15 m and 50 m.

The composite fuel moisture is set by the user, usually based on diagnosed 10 h dead fuel moisture at nearby Remote Automated Weather Stations (RAWS). This can be held steady for the experiment's duration or allowed to respond in a sinusoidal pattern with the average fuel moisture and amplitude set by the user. Treatments predicting the variation of fuel moisture have been presented (e.g. Nelson (2000)), but it is premature to implement them, because although increased fuel moisture is expected to reduce a fire's rate of spread, there is still no fundamental explanation for how fuel moisture affects the chemical reaction rates during combustion or decreases the rate of spread (Rothermel 1972; Sandberg et al. 2007). Because chaparral fuels have both living and dead components, we considered Fosberg and Schroeder's (1973) scheme to adjust dead fine fuel moisture to reflect the impact that the consumption of varying proportions of living herbaceous vegetation fuels may have on fire propagation. Ultimately, this was not applied as in many conditions it would have produced an adjusted fuel moisture that

exceeded the fuel moisture of extinction, and the fires would be predicted to not spread, when this is not the case. The role of chaparral's live component in fire propagation (or just how much is consumed) is still an active area of research (Zhou et al. 2007).

3.4 *Experiment design*

CAWFE can be configured in many different ways for different types of studies. It can be configured in LES mode to simulate at high resolution the interaction of a small fire with eddies in the atmospheric boundary layer. In that case, the atmospheric environment might be specified with an idealized profile or an atmospheric sounding.

For studying large wildfires, a simulation typically represents the meteorological flow preceding the ignition, the fire's ignition, growth while interacting with the atmospheric flow, and cessation. Using the initial conditions provided by the large-scale analyses or simulation, the simulation captures the atmospheric motions as modified by terrain before the fire's ignition. During this time, nested grid refinement refines the horizontal and vertical grid spacing to the resolution in the finest resolution modeling domain in which fire growth is modeled. Shear forces (such as those produced by topographic gradients or surface stresses that arise from surface roughness) or solar heating may be used to drive the turbulent boundary layer's development. At the reported ignition time, the simulation ignites a fire in the finest domain. The model simulates the remaining period of interacting weather and fire behavior.

Performing a mathematical difference of wind components between such a simulation with one in which a fire is not ignited allows one to determine to what extent the fire altered the atmospheric environment. Other sensitivity experiments can vary

parameters that are used in applying the fire's feedback to the atmosphere (α_s) and or the sensitivity to fuel parameters because these may affect simulations in a dynamic model differently than kinematic models such as FARSITE, amplifying or damping the model's response.

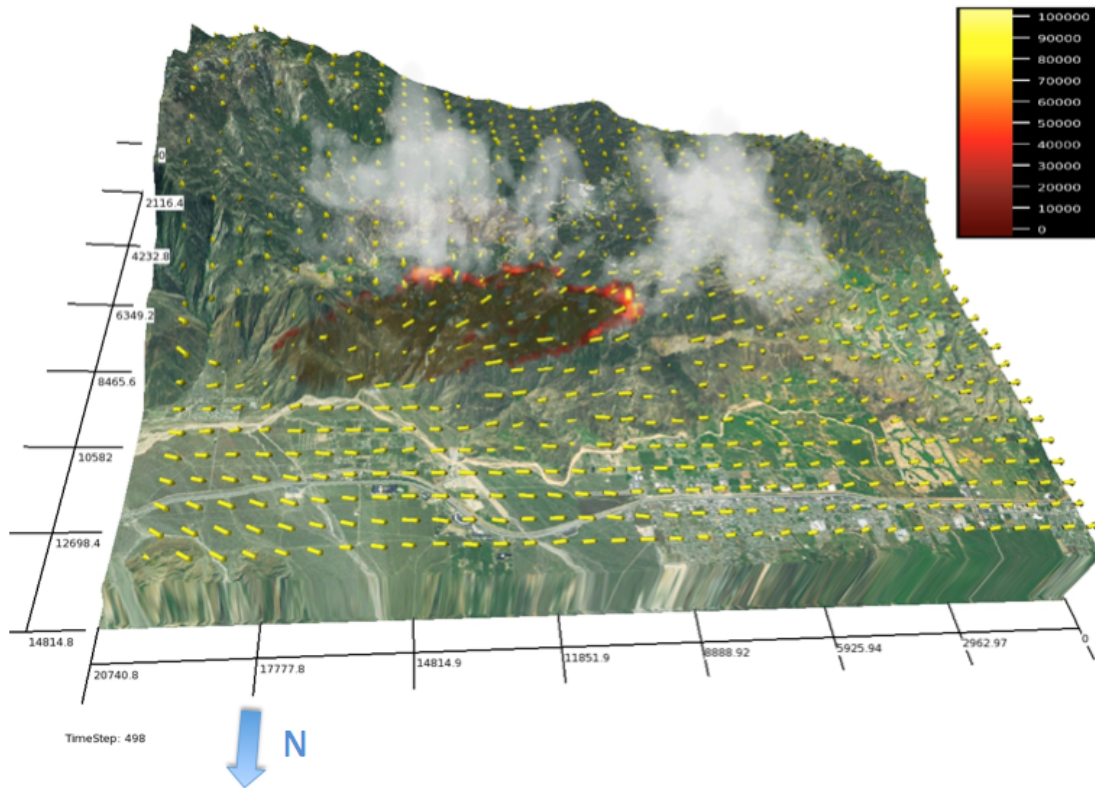


Figure 6. VAPOR visualization of the heat flux, near surface wind vectors, and smoke concentration during a CAWFE simulation of the 2006 Esperanza wildfire.

4. Model products

Standard analysis procedures for the Clark-Hall atmospheric model are described in Clark et al. (1996a). The addition of the fire behavior module adds several other fields to

the checkpointed model state files for restart and analysis, including two-dimensional variables such as sensible and latent heat fluxes on both the fuel and atmospheric grids, numerous fields that describe the location of tracers defining the fire line and that together outline the extent of the fire, remaining fuel loads, and a three-dimensional smoke mass concentration.

The model writes additional high frequency files containing a subset of these fields - dynamic variables, thermodynamic variables, smoke concentration, and the fire heat fluxes – for interactive scientific visualization packages such as Visualization and Analysis Platform for Ocean, Atmosphere, and Solar Researchers (VAPOR) (<http://www.vapor.ucar.edu/>). VAPOR creates and displays three-dimensional animations

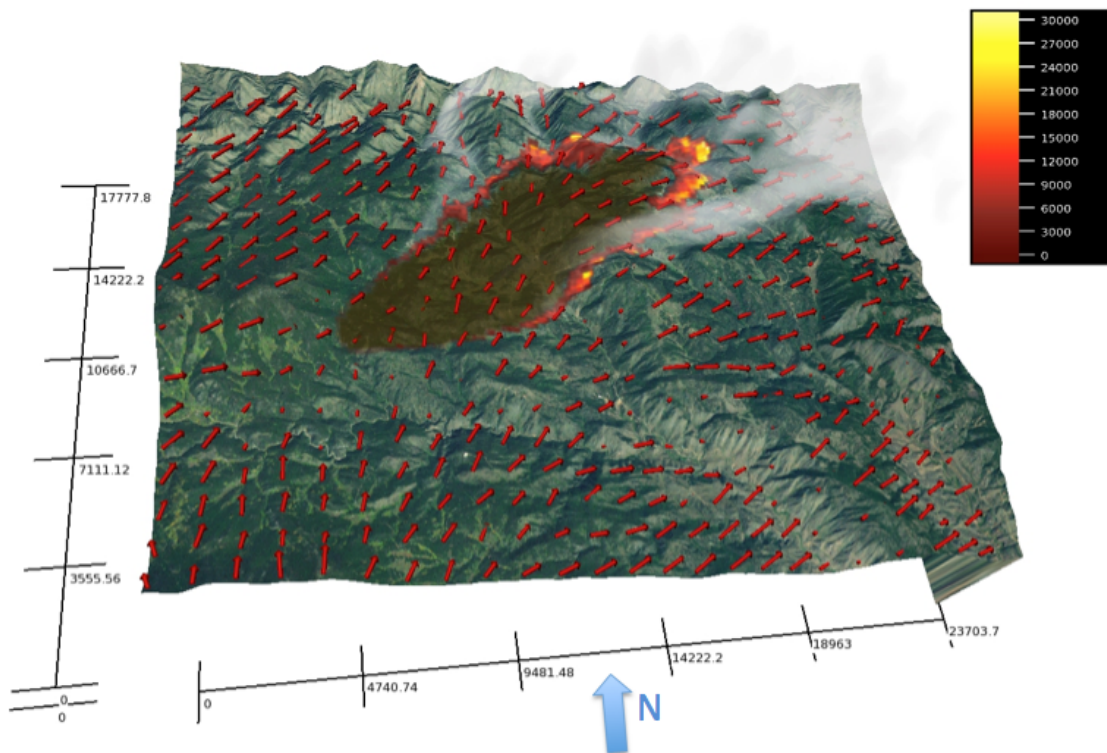


Figure 7. VAPOR visualization of the heat flux, near surface wind vectors, and smoke concentration during a CAWFE simulation of the 2012 High Park wildfire.

of geophysical datasets with the ability to view them over surface layers created from satellite, geopolitical, or geographical data. Using VAPOR, users can display and interact with four-dimensional CAWFE results such as the wind field, fire extent and heat fluxes, and smoke as they evolve before or during a fire event. Samples from previous CAWFE simulations of large fire events are shown in Figs. 6 and 7.

5. References

- Albini FA (1976) Estimating wildfire behavior and effects. USDA Forest Service Intermountain Forest and Range Experiment Station General Technical Report INT-30. (Ogden, UT)
- Albini FA (1994) PROGRAM BURNUP: A simulation model of the burning of large woody natural fuels. Final Report on Research Grant INT-92754-GR by USDA Forest Service to Montana State Univ., Mechanical Engineering Dept.
- Albini FA, Brown JK, Reinhardt ED, Ottmar RD (1995) Calibration of a large fuel burnout model. *International Journal of Wildland Fire* **5**, 173-192.
- Anderson HE (1982) Aids to determining fuel models for estimating fire behavior. USDA Forest Service, Intermountain Forest and Range Experiment Station General Technical Report INT-122. (Ogden, UT)
- Andrews PL (2009) BehavePlus fire modeling system, version 5.0: Variables. USDA Forest Service, Rocky Mountain Research Station General Technical Report RMRS-GTR-213WWW Revised. (Fort Collins, CO)
- Blackadar AK (1962) The vertical distribution of wind and turbulent exchange in a neutral atmosphere. *Journal of Geophysical Research* **67**, 3095– 3102.

- Clark TL (1977) A small-scale numerical model using a terrain following coordinate transformation. *Journal of Computational Physics* **24**, 186-215.
- Clark TL (1979) Numerical simulations with a three-dimensional cloud model: lateral boundary condition experiments and multi-cellular severe storm simulations. *Journal of Atmospheric Sciences* **36**, 2191-2215.
- Clark TL, Coen J, Latham D (2004) Description of a coupled atmosphere-fire model. *International Journal of Wildland Fire* **13**, 49–64
- Clark TL, Farley RD (1984) Severe downslope windstorm calculations in two and three spatial dimensions using anelastic interactive grid nesting: a possible mechanism for gustiness. *Journal of Atmospheric Sciences* **41**, 329-350.
- Clark TL, Hall WD (1991) Multi-domain simulations of the time dependent Navier Stokes equations: Benchmark error analyses of nesting procedures. *Journal of Computational Physics* **92**, 456-481
- Clark TL, Hall WD (1996) On the design of smooth, conservative vertical grids for interactive grid nesting with stretching. *Journal of Applied Meteorology* **35**, 1040-1046.
- Clark TL, Hall WD, Coen JL (1996a) Source code documentation for the Clark-Hall Cloud-scale model: Code version G3CH01. The National Center for Atmospheric Research (NCAR) Technical Note. NCAR/TN-426+STR. 174 pp.
- Clark TL, Jenkins MA, Coen J, and Packham D (1996b) A Coupled Atmospheric-Fire Model: Convective Feedback on Fire Line Dynamics. *Journal of Applied Meteorology* **35**, 875-901.

- Clark TL, Jenkins MA, Coen J, and Packham D (1996c) A Coupled Atmospheric-Fire Model: Convective Froude number and Dynamic Fingering. *International Journal of Wildland Fire* **6**, 177-190.
- Clark TL, Keller T, Coen J, Neilley P, Hsu H, Hall WD (1997) Terrain-induced Turbulence over Lantau Island: 7 June 1994 Tropical Storm Russ Case Study. *Journal of the Atmospheric Sciences* **54**, 1795-1814.
- Clements CB, Zhong S, Goodrick S, Li J, Potter BE, Bian X, Heilman WE, Charney JJ, Perna R, Jang M, Lee D, Patel M, Street S, Aumann G (2007) Observing The Dynamics Of Wildland Grass Fires: FireFlux: A Field Validation Experiment. *Bulletin of the American Meteorological Society* **88**, 1369-1382
- Coen JL (2005) Simulation of the Big Elk Fire using coupled atmosphere-fire modeling. *International Journal of Wildland Fire* **14**, 49–59.
- Coen JL, Cameron M, Michalakes J, Patton EG, Riggan PJ, Yedinak, KM (2013) WRF-Fire: Coupled Weather-Wildland Fire Modeling with the Weather Research and Forecasting Model. *J. Appl. Meteor. Climatol.* **52**, 16-38.
- Coen JL, Mahalingam S, Daily JW (2004) Infrared imagery of crown-fire dynamics during FROSTFIRE. *Journal of Applied Meteorology* **43**, 1241-1259.
- Finney MA (1998) FARSITE: Fire Area Simulator – model development and evaluation. USDA Forest Service, Rocky Mountain Station, Research Paper RMRS-RP-4, 47 pp.
- Fosberg MA, Schroeder MJ (1973) Fine herbaceous fuels in fire-danger rating. USDA Forest Service Research Note RM-185. 7 pp.

- LANDFIRE (2007) [Homepage of the LANDFIRE Project, U.S. Department of Agriculture, Forest Service; U.S. Department of Interior], [Online]. Available: <http://www.landfire.gov/index.php>.
- Lilly DK (1962) On the numerical simulation of buoyant convection. *Tellus* **14**, 145–172.
- Nelson RM Jr. (2000) Prediction of diurnal change in 10-h fuel stick moisture content. *Canadian Journal of Forest Research* **30**, 1071-1087.
- Noble IR, Bary GAV, Gill AM (1980) McArthur's fire danger meters expressed as equations. *Australian J. of Ecology*, **5**, 201–203.
- Ogura Y, Phillips NA (1962) Scale analysis of deep and shallow convection in the atmosphere *Journal of Atmospheric Sciences* **19**, 173-179.
- Oke TR (1987) Boundary Layer Climates. Methuen. 2nd Ed. London. 435 p.
- Riggan PJ, Wolden LG, Tissell RG, Coen J (2010) Remote sensing fire and fuels in southern California. Proceedings of 3rd Fire Behavior and Fuels Conference, October 25-29, 2010, Spokane, Washington. CD ROM. International Association of Wildland Fire. (Birmingham, AL) 14 pp.
- Rothermel RC (1972) A mathematical model for predicting fire spread in wildland fuels. USDA Forest Service, Intermountain Forest and Range Experiment Station, Research Paper INT-115. (Ogden, UT)
- Sandberg DV, Riccardi CL, Schaaf MD (2007) Reformulation of Rothermel's wildland fire behaviour model for heterogeneous fuelbeds. *Canadian Journal of Forest Research* **37**, 2438–2455.
- Scott JH, Burgan RE (2005) Standard fire behavior fuel models: a comprehensive set for use with Rothermel's surface fire spread model. USDA Forest Service, Rocky

Mountain Research Station, General Technical Report RMRS-GTR-153. (Fort Collins, CO)

Smagorinsky J (1963) General circulation experiments with the primitive equations.

Proceedings of the International Symposium on Numerical Weather Prediction, Tokyo, Japan, Meteor. Soc. Japan, 85–107.

Van Wagner CE (1977) Conditions for the start and spread of crown fire. *Canadian*

Journal of Forest Research **7**, 23-34.

Wilson R (1980) Reformulation of fire spread equations in SI units. USDA Forest

Service, Intermountain Forest & Range Experiment Station, Research Note INT-292. (Ogden, UT)

Zhou X, Mahalingam S, Weise D (2007) Experimental study and large eddy simulation

of effect of terrain slope on marginal burning in shrub fuel beds. *Proceedings of the Combustion Institute* **31**, 2547-2555.